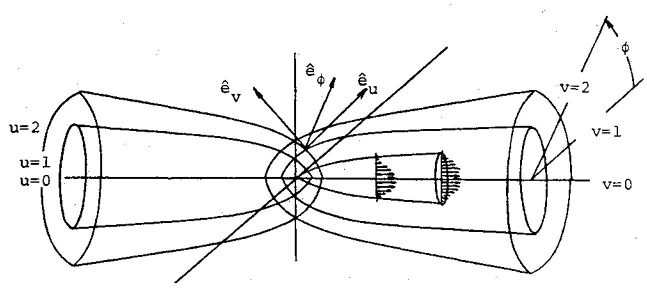

Fig. 1 Round jet in paraboloidal coordinates.

substitutions reproduce the results of classical boundary-layer theory, i.e., $\epsilon = 1/\sqrt{Rey}$. Thus, it is seen that to first order, taking $P^* \equiv P_\infty$, the governing equations reduce to, returning to dimensional quantities,

$$AA_u + BA_v = \frac{\nu}{u^2 v}(uvA_v)_v \tag{6a}$$

$$(u^2 vA)_u + (u^2 vB)_v = 0 \tag{6b}$$

The "modified" continuity equation (6b) now may be integrated by the introduction of a stream function Ψ^i defined by $u^2vA = \Psi^i_v$ and $u^2vB = -\Psi^i_u$ where subscripts again denote partial differentiation. The momentum equation (6a) is thereby transformed to

$$\Psi^i_v \frac{\partial}{\partial u}\left(\frac{1}{u^2 v}\frac{\partial \Psi^i}{\partial v}\right) - \Psi^i_u \frac{\partial}{\partial v}\left(\frac{1}{u^2 v}\frac{\partial \Psi^i}{\partial v}\right) = \nu\frac{\partial}{\partial v}\left(uv\frac{\partial}{\partial v}\frac{1}{u^2 v}\frac{\partial \Psi^i}{\partial v}\right) \tag{7}$$

It is apparent from dimensional considerations that the integration of Eq. (7) may be more easily accomplished by taking $\eta = v/u$ as an independent variable and by taking Ψ^i in the form $\Psi^i = \nu u^2 f(\eta)$. With this assumption, the conditions of symmetry and finite velocity along the jet axis requires $f(0) = 0$. The condition of zero flow far from the jet axis requires that $f'(\infty) = f''(\infty) = 0$. The latter boundary conditions (at infinity) are not independent of each other; still another condition needs to be prescribed. Physically, this condition is related to the strength of the jet; the constant associated with this integration is analagous to the α of Sec. I.

Equation (7) may now be cast into the more simplified form

$$f''' - \frac{1}{\eta}f'' + \frac{1}{\eta^2}f' = \frac{2}{\eta^2}ff' - \frac{2}{\eta}ff'' - \frac{2}{\eta}(f')^2 \tag{8}$$

or, alternatively,

$$(f'')' - (f'/\eta)' = -2(ff'/\eta)'$$

Here, the primes indicate differentiation with respect to η. Successive integrations yield

$$(2ff' + \eta f'' - f')/\eta = \gamma \qquad \text{with } \gamma = 0$$

$$\eta f' + f^2 - 2f = \beta \qquad \text{with } \beta = 0$$

and, finally,

$$f = 2\eta^2/(\eta^2 + \kappa)$$

Thus, the first-order boundary-layer solution is given by

$$\Psi^i = 2\nu u^2 \eta^2/(\eta^2 + \kappa) \tag{9}$$

where κ is related to the momentum strength (or jet width). I is an easy matter to establish the relation $\alpha = 2\kappa$ from simpl coordinate transformations; then, Eqs. (3) and (4) are ex pected to remain valid so that the flow is completely deter mined when M, F, or $M+F$ are specified.

For the outer flow, the independent variables of Eqs. (5a-c do not require stretching; consequently, to first order, on recovers the inviscid Euler equations. The solution to thi order, because the flow is irrotational far upstream, satisfie $\nabla \times \hat{q} = 0$. This condition, together with a definition of stream function Ψ^0 appropriate to Eq. (5c), i.e., $uvA/R = \Psi$ and $uvB/R = -\Psi^0_u$, determines the governing potential flo equation

$$\Psi^0_{uu} + \Psi^0_{vv} - \Psi^0_u/u - \Psi^0_v/v = 0 \tag{1C}$$

The corresponding ("line sink") boundary condition on th jet axis is obtained from the limit matching principle. Henc it is required that $\lim_{v\to 0}\Psi^0 = \lim_{\eta\to\infty}\Psi^i$, i.e., $\Psi^0(v=0) = 2\nu u^2$ In addition, the solution to Eq. (10) must satisfy the conditio of zero flow far from the jet axis. The outer (potential) flo solution in this case is obviously given by the inner boundar condition; that is, $\Psi^0(u,v) = 2\nu u^2$. (This, of cours reproduces the fact that the outer stream surfaces ar paraboloidal.)

III. Conclusion

It is seen from the results of Sec. II that the composi solution $\Psi^c = \Psi^i + \Psi^0 - 2\nu u^2$ is identical to Ψ^i. Thus, for th laminar round jet problem, an optimal coordinate system h been discovered. It has been shown by Kaplun[1] that in th case of planar flows, optimal coordinates are not unique. I the general case, such coordinates are not expected to coinci with streamline coordinates. The results of this paper sugge that, for Squire's jet, the connection between the two types coordinate systems is stronger. For further discussion o optimal coordinates, the reader is referred to Ref. 6.

References

[1]Kaplun, S., "The Role of Coordinate Systems in Boundary La Theory," *Z. Angew. Math. Phys.*, Vol. 5, 1954, pp. 111-135.
[2]Batchelor, G. K., *An Introduction to Fluid Dynamics*, Cambrid University Press, London, 1967.
[3]Yih, C. S., *Fluid Mechanics*, McGraw-Hill, New York, 1969.
[4]Squire, H. B., "The Round Laminar Jet," *Quarterly Journal Mechanics and Applied Mathematics*, Vol. 4, 1951, pp. 321-329.
[5]Coles, D., "Lecture Notes on Advanced Fluid Mechanics 201," California Institute of Technology, Pasadena, Calif., 1972.
[6]Van Dyke, M., *Perturbation Methods in Fluid Mechani* Academic Press, New York, 1964.

AIAA 81-4015

A Study of Multiple Jets

S. Raghunathan* and I. M. Reid†
Queen's University, Belfast, Northern Ireland

Nomenclature

D_0	= diameter of a single jet, 3.57 mm
f	= octave band center frequency
m	= jet momentum
R	= radial distance from the jet(s) central axis
$R_{1/2}$	= radial distance at which the velocity is half central velocity
S	= Strouhal number, fD_0/V_j

Received July 7, 1980.
*Lecturer, Department of Aeronautical Engineering.
†Formerly, Student, Department of Aeronautical Engineering.

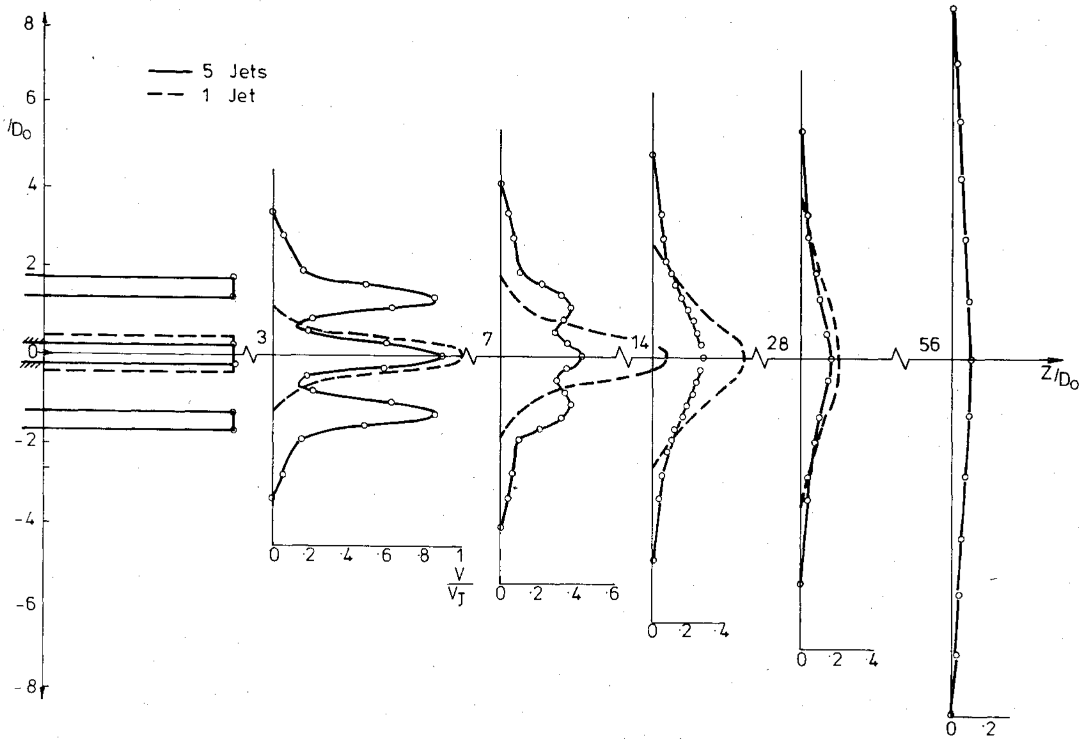

Fig. 1 Velocity profiles for single and multiple jets.

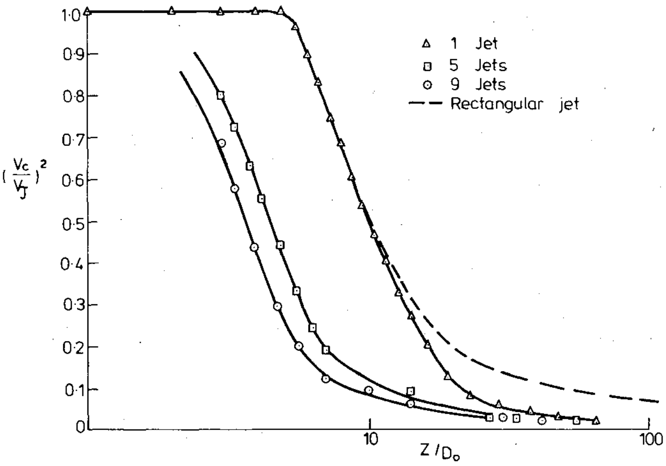

Fig. 2 Decay of axial jet velocity.

SPL = sound pressure level, dB (ref. 2×10^{-5} N/m^2)
V = velocity in the jet
V_c = jet(s) centerline velocity
V_j = jet(s) exit velocity
Z = axial distance along the jet axis

Introduction

THE use of multiple jets to attenuate the jet noise of aircraft is well known.[1] Multiple jets, rectangular and circular, in an array with and without ejector shrouds have been a subject of recent investigation.[2,3] Jets are also used in industries in a variety of situations. Noise from such jets is an important factor in industrial noise control. These jets usually operate at a supply pressure of 0.3-0.5 MPa (3-5 bar) and the momentum and turbulence of the jet are important in cleaning and dispersing the materials. It should be possible to reduce the noise level of a jet by using multiple jets; however, the effect of such a system on the momentum of the jet is not clearly understood. There is no information available on the structure of multiple jets with the jets arranged around a central axis and operating at a supply pressure 0.3-0.5 MPa (3-5 bar). This Note presents certain characteristics of such jets.

The Tests

The test setup consisted of a compressed air supply, a filter, a settling chamber, and a nozzle plate holder onto which was connected one of four interchangeable circular plates with a different number of nozzles on each (1, 5, 7, and 9). The multiple nozzles were equally spaced around a circle with a radius of 5 mm from the axis of the central nozzle. The total nozzle area on each plate was kept constant at 9.75 mm^2. The area ratio between the reservoir and the nozzles was 52. All of the nozzles were operated at a constant pressure difference of 207 kPa (30 psi) between the settling chamber and the ambient, resulting in a jet velocity of 520 m/s. The test setup was located in a large semireverberant room.

Measurements were made of velocity profiles and thrust at several positions along the jet central axis. A pitot tube with a frontal opening area of 0.5 mm^2 was used for the velocity measurements. A flat plate with a balance, the sensitivity of which was 0.01 N, was used for the thrust measurements. Measurements were also made for the noise levels at several locations around the jet. A CEL 175 noise meter with an octave band filter was used for this purpose.

Results

Figure 1 compares the nondimensional velocity profiles for a single jet with those of a multiple jet. Profiles are shown for the nozzle exit and for four values of Z/D_0. It is observed with the merging of velocity profiles that there is an interaction between the profiles, with the peak velocities of the outer jets shifting toward the central axis. At a value of $Z/D_0 = 14$, the multiple jets have merged together to form a single jet. Improved mixing in the case of multiple jets results in a rapid decrease in peak velocities. At about $Z/D_0 = 56$ the differences between the multiple and single jets are not noticeable, either in terms of velocities or the extent of radial spread.

A plot of $(V_c/V_j)^2$ vs Z/D_0 is shown in Fig. 2 to indicate the decay of the axial velocity of the jet. Increasing the number of jets increases the decay of the axial velocities. Significant decay occurs between $Z/D_0 \simeq 5$ and $\simeq 20$ for a

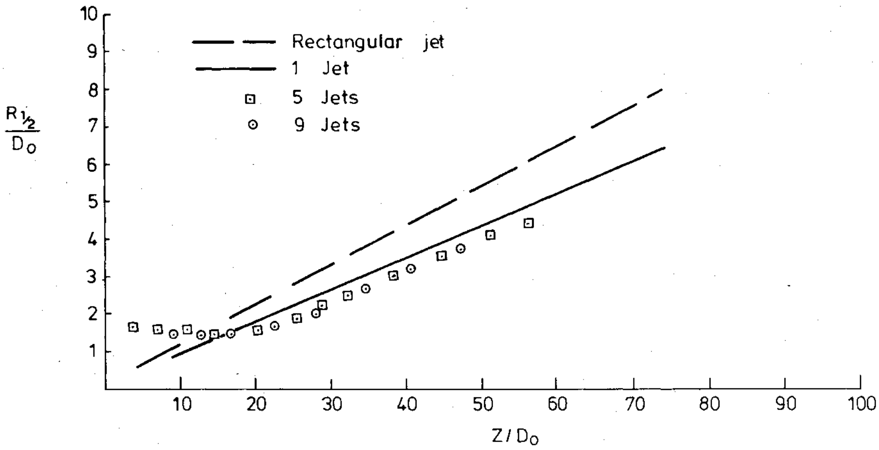

Fig. 3 Jet boundary.

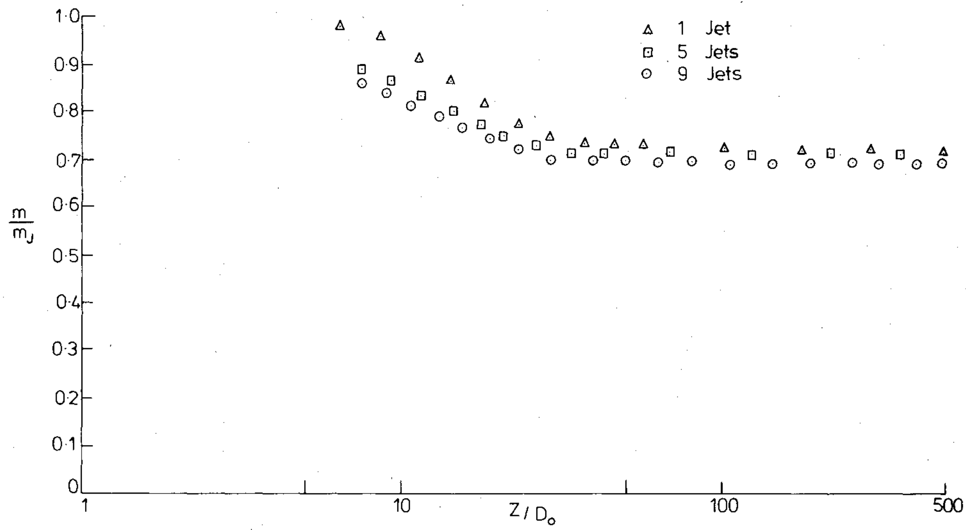

Fig. 4 Variation of jet momentu with axial distance.

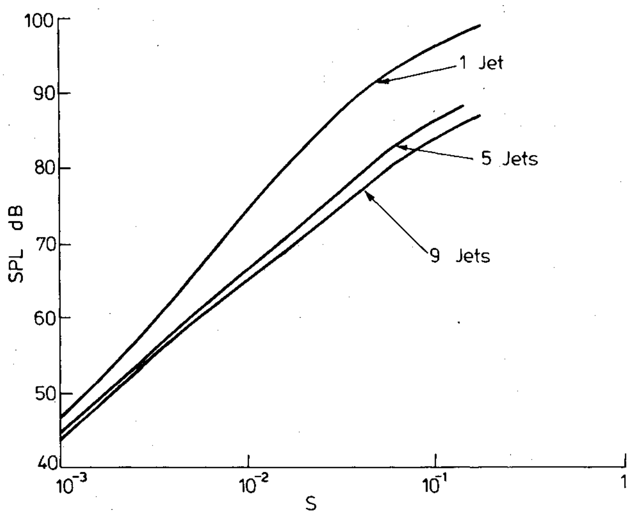

Fig. 5 Noise spectra of multiple jets.

single jet. The corresponding values for nine jets are $Z/D_0 \simeq 2$ and $\simeq 10$. The value of $(V_c/V_j)^2$ reaches less than 2% at $Z/D_0 \simeq 50$ for both single and multiple jets. A curve for a rectangular jet is also shown for comparison. A rectangular jet takes a longer distance to decay.

The spread of jets in the R-Z plane is shown in Fig. 3. Here $R_{½}$ is the radius at which the velocity in the jet is half the centerline velocity. Using this criterion to express the spread of the jet avoids the difficulty in precisely locating the boundary of the jet. A single jet shows a linear growth, th growth rate corresponding to a total spread angle of 10 de The growth rate of multiple jets is negligible up to a distanc $Z/D_0 \simeq 20$ after which the growth closely follows that for single jet.

The variation of jet momentum with the axial distance shown in Fig. 4. The momentum generally drops to a valu about 75% of the initial value at $Z/D_0 \simeq 20$, after which tends to assume a value of about 70% and this is maintaine even at a distance $Z/D_0 = 500$. The momentum of multip jets is generally lower than that for a single jet by about 10 at $Z/D_0 = 10$ and by about 5% at $Z/D_0 \simeq 500$ for the nine-je case.

The main advantage of the multiple-jet system is seen by t noise reduction shown in Fig. 5. The spectra shown here a based upon an octave bandwidth and measured at a point 1 m from the jet exit and on a line 30 deg from the jet axis. T spectra peak at a Strouhal number of $n \simeq 0.2$ whic corresponds to $f = 20$ KHz. Frequencies greater than 20 KH would not be of much interest in noise control. Substanti reduction in noise level for the five-jets case is clearly see The reduction in noise level by increasing the number of je above five is rather small.

It does appear that a multiple-jet nozzle with five jets offe an advantage in terms of noise reduction without significa reduction in the momentum of the jet. Further experiments determine the turbulence structure of the jets are in progress

Acknowledgment

The authors wish to thank Prof. E. J. Richards Southampton University for his help and advice.

References

[1]Tyler, J. M., "Jet Engine Noise and its Control," AGARD LS 77, 5-1, 1977.

[2]Bocher, I. V., "Noise and Flow Characteristics of Linear Array of Jets and Ejector Flow Systems," Ph.D. Thesis, University of Tennessee, Knoxville, 1976.

[3]Krothapalli, A., "An Experimental Study of Multiple Jet Mixing," Ph.D. Thesis, Stanford University, Stanford, Calif., 1979.

AIAA 81-4016

Pulsed Laser Propulsion

P. E. Nebolsine,* A. N. Pirri,† J. S. Goela,‡ and G. A. Simons§

Physical Sciences Inc., Wolburn, Mass.

I. Introduction

EXPERIMENTS have been carried out to assess the performance of a rocket propelled by absorption of radiant energy from a remotely stationed, repetitively pulsed laser. The concept, deceptively simple, is to provide a high-energy density for propulsion without the encumbrance of a massive on-board energy source by absorbing radiation from a remotely stationed high-powered laser. Since the radiation-absorbing propellant may be a high-temperature plasma, the specific impulse can be very large (i.e., >1000 s), and the available laser power will limit the achievable thrust. Larger payload/vehicle weight ratios are clearly possible with a 1000 s specific impulse laser-powered rocket than with chemical propulsion rockets. In the following sections a theoretical update[1] and extension of previously analyses[2] to 1 atm operation of such a device are provided; experimental results for both 1 atm and vacuum environments are presented.

II. Theoretical Studies

A fluid mechanical model has been developed to assess the performance of the laser-powered thruster concept in a vacuum environment utilizing blast-wave theory to calculate the thrust and specific impulse.[2] When the pulsed laser-powered thruster operates in a finite-pressure environment, the laser requirements are altered by two effects. First, propellant flow into the nozzle is characterized as flow through a highly overexpanded nozzle. A normal shock stands close to the nozzle's throat (prior to laser breakdown), and most of the flow is subsonic in the nozzle's diverging section. This results in a reduction of the repetition frequency necessary to attain a given specific impulse. In addition, since background pressure reduces the propellant expulsion velocity after breakdown, it is possible for shocks from subsequent laser breakdowns to propagate into the hot propellant from a previous laser pulse. It has been shown[1] that the specific impulse, I_{sp}, obtained for operation in a background gas be related to the vacuum specific impulse by

$$I_{sp} = \frac{3}{4}\frac{t_{conv}}{\Delta t}\,[I_{sp}]_{vac,\,\Delta t = t_{conv}} \tag{1}$$

Received Jan. 21, 1980; revision received June 2, 1980.

*Manager of Experimental Research.

†Manager of Laser Applications. Member AIAA.

‡Principal Scientist.

§Principal Scientist. Member AIAA.

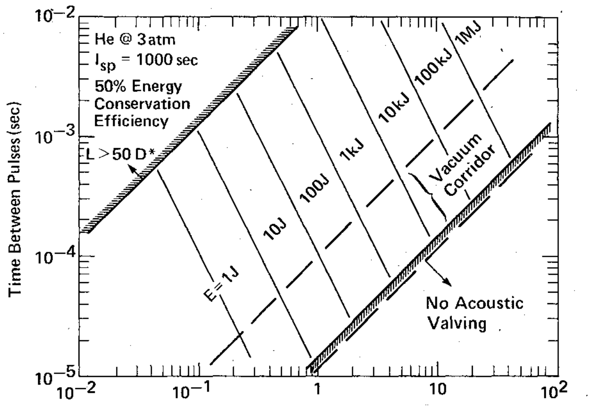

Fig. 1 Laser energy requirements, 1 atm background.

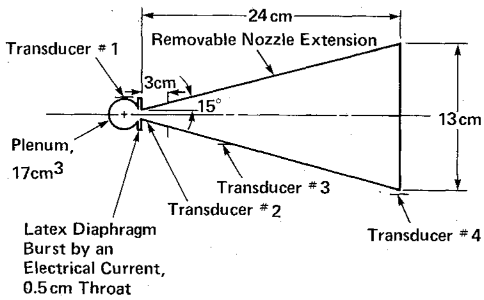

Fig. 2 Conical nozzle design.

where t_{conv} is the time it takes the unshocked propellant to reach the exhaust plane in ambient gas environment, Δt is the time between pulses, and $[I_{sp}]_{vac,\,\Delta t_{conv}}$ is the calculated vacuum specific impulse when the time between pulses Δt is set equal to the convection time. Laser energy requirements for operation in a 1 atm background gas are mapped in Fig. 1. The operating corridor is delineated between the shaded zones. The limits are provided by acoustic valving and an expansive nozzle length (L) to throat diameter ratio (D^*).[1,2] Shorter nozzles and slower repetition rates are required for operation in a 1 atm environment than in a vacuum (see Fig. 10 of Ref. 1).

III. Experimental Studies

Using the theory just summarized to design the nozzle and laser system parameters, we have performed small-scale experiments to 1) verify theoretical predictions of high specific impulse obtainable with the pulsed laser-powered thruster concept, 2) measure time-averaged specific impulse and thrust vs laser parameters, and 3) study the effect of finite exit plane pressure on thrust and specific impulse. The experiments were carried out using several independently triggered 10.6 μm CO_2 TEA lasers (Lumonics, Model 103). Each laser delivers up to 11 J in energy over a pulse time of approximately 3 μs. Two nozzle geometries were investigated. A conical nozzle was used first for direct comparison with the theory. Each laser beam was focused externally with 30 cm focal length mirrors into the nozzle, resulting in a focal point at the throat. A schematic of the conical nozzle design is shown in Fig. 3. The length shown is the design length for vacuum operation. However, since nozzle length for 1 atm operation is less than 4 cm, the nozzle skirt was constructed in removable sections. A self-contained plenum attached to the nozzle contains sufficient propellant for operation with up to four laser pulses with a plenum pressure drop of less than 10%. A latex diaphragm was used to maintain plenum pressure at 3 atm until the experiments began, and a spark was used to break the diaphragm. Lasers were triggered in